ACES Asian Chemical Editorial Society

doi.org/10.1002/ajoc.202100373

ASIAN JOURNAL OF ORGANIC CHEMISTRY
Full Paper

Synthesis of 5-Azatetracene and Comparison of Its Optical and Electrochemical Properties with Tetracene

Animesh Ghosh,[a] Maja Budanovic[+],[b] Tianjiao Li[+],[c] Caihong Liang[+],[a] Maciej Klein,[d, e] Cesare Soci,[d] Richard D. Webster,[b] Gagik G. Gurzadyan,*[c] and Andrew C. Grimsdale*[a]

Abstract: A four-step route for the synthesis of 5-azatetracene (benzo[b]acridine) has been developed, employing a base-catalysed Friedlander condensation reaction between 3-amino-2-napthaldehyde and cyclohexanone as the key step followed by dehydrogenation of the intermediate. The optical and electrochemical properties of the 5-azatetracene were investigated by UV-vis and photoluminescence spectroscopy, and by cyclic voltammetry and compared with those of tetracene. It is found that 5-azatetracene shows broader absorption in the visible region than tetracene, exhibits a higher luminescence quantum efficiency, and possesses a lower-lying LUMO level and smaller HOMO-LUMO band gap. Time-resolved PL spectroscopy was used to elucidate the reasons for the more efficient luminescence of 5-azatetracene. Field-effect transistor measurements revealed the ambipolar nature of charge transport in 5-azatetracene.

Introduction

Over the last decade, acenes have gained considerable attention as charge-transport materials in transistors and other electronic devices. Acene derivatives, such as rubrene (**1**) or TIPS-pentacene (**2**), due to their extended π-conjugation and efficient molecular packing, exhibit excellent hole transporting behavior (p-type) and have been used extensively as active components in organic electronic devices.[1–5] While carbocyclic acenes exhibit p-type character, with the advent of novel organic synthesis methodologies, a lot of effort has been devoted to tune the electronic structures and properties of π-conjugated frameworks of acenes by replacing CH groups with heteroatoms such as N, B, S, P etc.[6–15] The resulting heteroacenes are structurally similar to their hydrocarbon analogues, but the heteroatoms alter the energy levels of the frontier molecular orbitals (FMOs) and can affect the intermolecular packing. In particular, nitrogen containing heteroacenes have been shown to be promising electron-transporting materials, as replacement of a benzene ring with pyridine or pyrazine rings to form N-heteroacenes increases their electron affinity. In recent years, a number of N-heteroacenes, e.g. TIPS-functionalized tetraazapentacene (**3**), have been reported to exhibit good electron mobility, and so can be used to fabricate n-type thin-film transistors.[16–19] Heteroacenes also have been reported to display good photoluminescence properties and high singlet fission cross-sections, making them promising compounds for other applications.[20–22] In recent years, many azaacenes have been prepared by many methods, and their properties have been investigated by various spectroscopic methods and by electrochemistry.[23–28] The optical and electrochemical properties of N-heteroacenes depend upon position and number of nitrogen atoms. Miao and co-workers demonstrated that azaacenes containing nitrogens on internal rings exhibit lower FMO energies than their analogues with terminal heterocyclic rings.[20] The majority of the reported N-heteroacenes contain 1 or 2 pyrazine rings in their backbones, since these can be conveniently synthesized by conventional condensation reactions or by palladium-catalyzed Buchwald coupling reaction, with little work reported on heteroacenes containing pyridine rings, though these also have shown some promising properties. For example, the diazapentacenes **4** (obtained as an inseparable 1:1 mixture of **4a** and **4b**) are reported to show efficient ambipolar charge transport,[23] and promising singlet fission properties.[29] Due to the small number of such materials that have been made, there is a lack of experimental data from which to derive structure-property relationships to determine how the introduction of nitrogen atoms at individual sites in acenes can affect their optoelectronic properties. As part of an effort to fill in this gap in our knowledge of heteroacenes, we

[a] *Dr. A. Ghosh, C. Liang,[+] Prof. A. C. Grimsdale*
School of Materials Science and Engineering
Nanyang Technological University
50 Nanyang Avenue, 639798 (Singapore)
E-mail: acgrimsdale@ntu.edu.sg

[b] *Dr. M. Budanovic,[+] Prof. R. D. Webster*
Division of Chemistry and Biological Chemistry, School of Physical and Mathematical Sciences
Nanyang Technological University
21 Nanyang Link, 637371 (Singapore)

[c] *T. Li,[+] Prof. G. G. Gurzadyan*
Institute of Artificial Photosynthesis, State Key Laboratory of Fine Chemicals
Dalian University of Technology
2 Linggong Road, Dalian, 116024 (P. R. China)
E-mail: gurzadyan@dlut.edu.cn

[d] *Dr. M. Klein, Prof. C. Soci*
Division of Physics and Applied Physics, School of Physical and Mathematical Sciences
Nanyang Technological University
21 Nanyang Link, 637371 (Singapore)

[e] *Dr. M. Klein*
Energy Research Institute @ NTU (ERI@N), Research Techno Plaza
Nanyang Technological University
50 Nanyang Drive, 637553 (Singapore)

[+] *These authors contributed equally to this work.*

Supporting information for this article is available on the WWW under https://doi.org/10.1002/ajoc.202100373

have recently reported routes to prepare derivatives of 5,7-diazapentacene such as **5** (Figure 1).[30–31]

In this work, we report the synthesis of 5-azatetracene (benzo[b]acridine, **6**) by means of a Friedländer condensation followed by dehydrogenation, and on a study of its electrochemical and optical properties, and how they compare with those of tetracene (**7**). The synthesis of **6** has been previously reported by a number of routes,[32–33] but no investigation of its optical and electrochemical properties has been reported. There is no report of its synthesis by a route involving a Friedländer reaction of an α-aminobenzaldehyde, though it has been made by the reaction of naphthyne (generated in situ from 2,3-naphthoxadisilole) with 2-aminobenzaldehyde.[32] We postulated that a viable route to **6** would be the Friedländer reaction of 3-amino-2-napthaldehyde with cyclohexanone, followed by aromatization (Scheme 1), especially since a similar route for the synthesis of 5-azapentacene is reported elsewhere.[34]

Results and Discussion

Synthesis

The synthetic route to preparation of **6** is outlined in Scheme 1. 3-Amino-2-napthaldehyde **8** was synthesized from 3-amino-2-napthoic acid (**9**) in 36% yield in two steps following a literature procedure.[35] The o-amino aldehyde **8** was next subjected to a base catalysed Friedlander reaction[36–41] to provide 1,2,3,4-tetrahydrobenzo[b]acridine **10** in 83% yield. Finally, **10** was aromatized by heating at 150 °C in nitrobenzene with 10% Pd/C[42] to provide the desired product **6** in 39% yield. The overall yield from **9** is 12%. This is lower than the overall yields for the synthesis of **6** via naphthyne addition to aminobenzaldehye (16%)[32] and via a copper-catalysed additon of a ketone to a diaryldibromide (34%)[33] but involves less steps than the former and is experimentally less demanding than the latter. There exists scope for improvement of the yield as the aromatisation

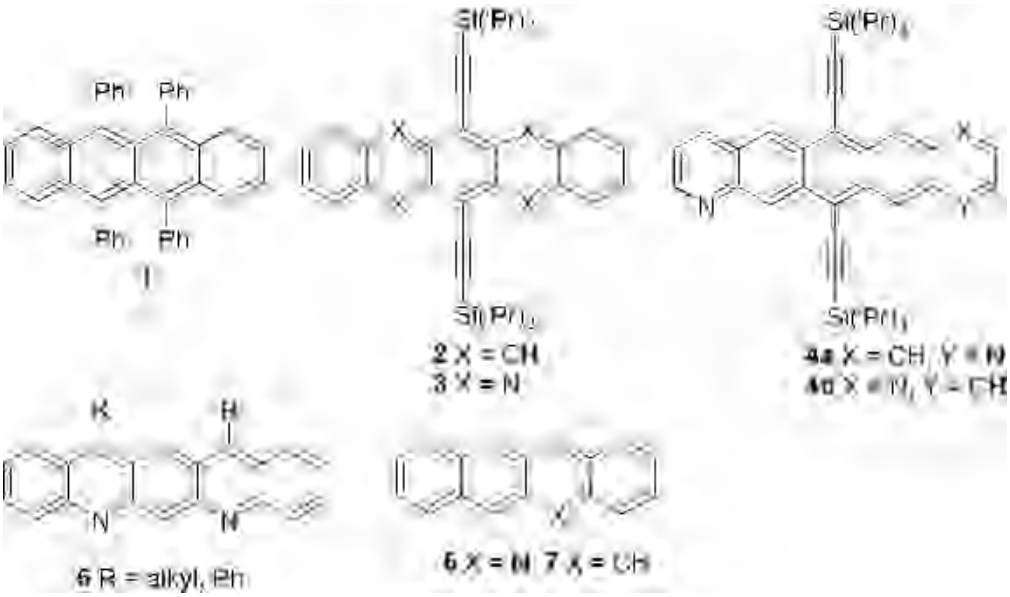

Figure 1. Chemical structures of acenes and heteroacenes.

Scheme 1. Synthesis of 5-azatetracene (**6**).

step has not been optimised and this route should be facilely extended to make substituted azatetracene derivatives.

Optical and electronic properties

Photographs of the dichloromethane solutions of 5-azatetracene **6** and tetracene **7** are shown in Figure 2. In ambient light, the solutions of **6** and **7** are orange and yellow respectively. Under illumination with ultraviolet light (365 nm), **6** shows strong yellow fluorescence while **7** shows light blue fluorescence.

The optical properties of **6** were studied in dichloromethane solution by UV-vis absorption and photoluminescence spectroscopy and compared with those of tetracene. The replacement of CH with an N atom increases the π-conjugation in the 5-azatetracene backbone and is expected to stabilize the frontier molecular orbitals (FMOs) and lower the optical band gap. While tetracene showed the first absorption maxima at 474 nm, it is bathochromically shifted by 60 nm in 5-azatetracene [534 nm] (Figure 3). The band gap of 5-azatetracene (2.00 eV), determined from the edge of absorption spectrum, is smaller than that of tetracene (2.54 eV) (Table 1).[43] The smaller bandgap in **6** is consistent with the expected changes in the FMOs due to the presence of the heteroatom. The UV-vis absorption in solid state was investigated on thin films prepared by drop casting on quartz slide from chloroform solution (Figure S1). The UV-vis spectra of tetracene exhibits a

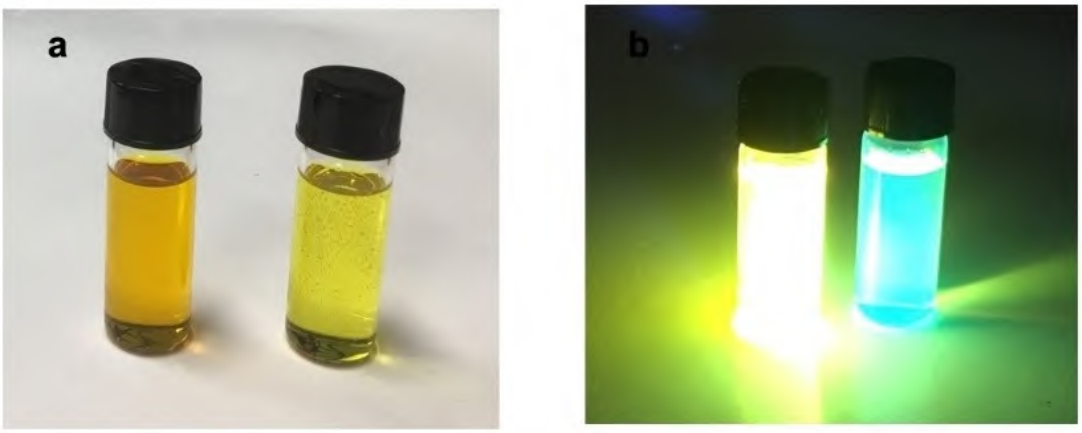

Figure 2. Photographs of 5-azatetracene (left) and tetracene (right) (a) in ambient light and (b) in dark with irradiation at 365 nm.

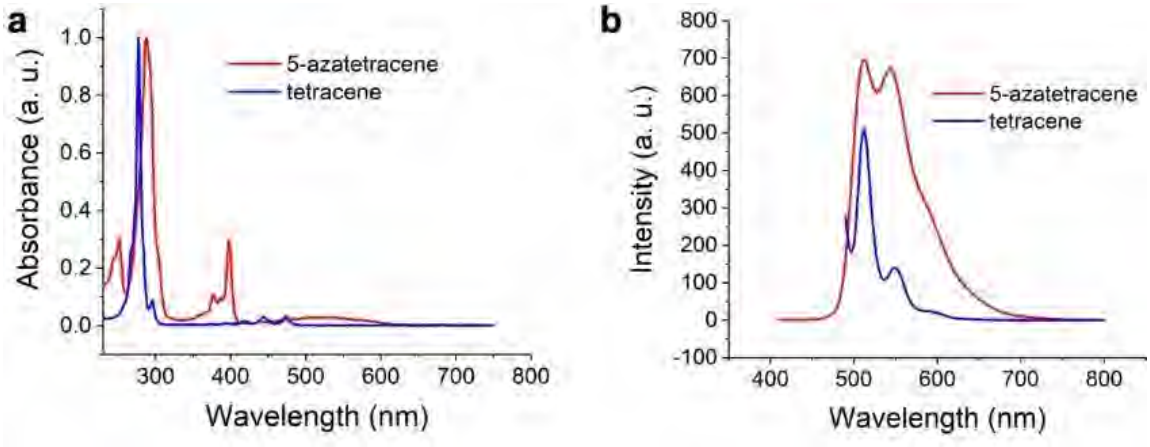

Figure 3. (a) Normalized UV-vis absorption and (b) normalized fluorescence spectra of 5-azatetracene (red) and tetracene (blue) in dichloromethane solution.

Table 1. Optical data of 5-azatetracene (**6**) and tetracene (**7**).

Compound	$\lambda_{abs,\,max}$ [nm][a]	λ_{onset} [nm]	λ_{ex} [nm]	λ_{em} [nm][a]	ΔE_g^{opt} [eV][b]	Φ[c]
6	534, 397, 376	620	397	544, 513	2.00	0.63
7	474, 444, 295	487	474	550, 512	2.54	0.10

[a] Measured in dichloromethane solution. [b] Estimated using the onset of the UV-vis spectrum in solution by $E_g^{opt} = 1240/\lambda_{onset}$. [c] Measured in chloroform solution.

broad peak at 516 nm in addition to the peak at 474 nm, which is consistent with an earlier report.[44] The UV-vis spectra of 5-azatetracene exhibits a peak at 522 nm, which is blue-shifted by 12 nm in comparison to that in solution.

Emission spectra of both tetracene and 5-azatetracene in dichloromethane solution showed two peaks at λ_{em} (550 nm, 512 nm) and at (544 nm, 513 nm) respectively. First emission peak of 5-azatetracene exhibited much higher intensity with an enhanced quantum yield value ($\Phi = 0.63$), while the measured quantum yield of tetracene is $\Phi = 0.10$ (Table 1).

In order to explore the origin of emission in tetracene and 5-azatetracene, time-correlated single photon counting (TCSPC) technique was applied with $\lambda_{ex} = 380$ nm and the resulting fluorescence kinetics of tetracene and 5-azatetracene in dichloromethane are presented in Figure 4. The emission of tetracene and 5-azatetracene exhibits monoexponential decay with $\tau = 2.6$ and 11 ns, respectively, originating from the locally excited singlet state S_1. These are in good agreement with the steady-state fluorescence quantum yields $\Phi = 0.10$ and $\Phi = 0.63$, as we assume that the radiative lifetimes (ratio of the fluorescence lifetime and the fluorescence quantum yield) are approximately equal for tetracene and 5-azatetracene. Fluorescence maps (Figure 5) of tetracene and 5-azatetracene in dichloromethane solution at $\lambda_{ex} = 380$ nm are similar to the steady-state emission spectra (Figure 3b). The replacement of CH with N atom increases the π-conjugation in the 5-azatetracene backbone leads very strong fluorescence in comparison to tetracene. More clearly, fluorescence maps of tetracene and 5-azatetracene in dichloromethane show the same trend as discussed above, i.e. in 5-azatetracene emission is stronger. This comparison indicates the importance of N substitution in 5-azatetracene in modulating the optical properties of tetracene.

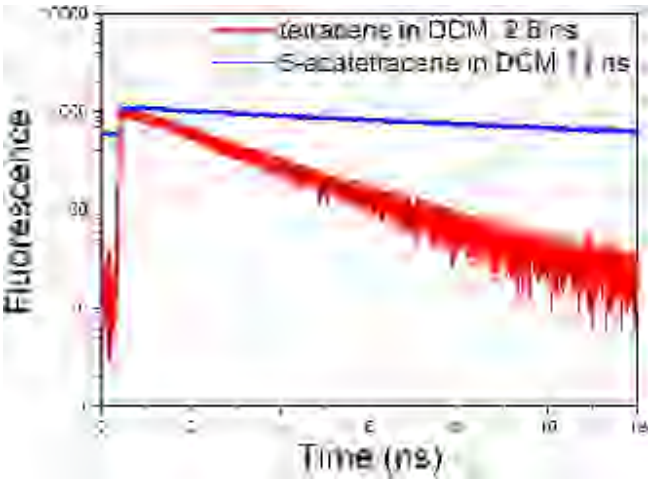

Figure 4. Fluorescence decay kinetics at 500 nm of tetracene and 5-azatetracene in dichloromethane solution, $\lambda_{ex} = 380$ nm.

The marked difference in photoluminescence quantum yield (PLQY) between tetracene and 5-azatetracene in solution might be attributable to the relative alignment between the singlet (S_1) state and triplet (T_2) state energies, as has been shown for rubrene and other tetracene derivatives.[13,45] However, according to our calculations the T_2 state of tetracene (and also of 5-azatetracene) is well above the S_1 state (Table S1), which is in agreement with literature data.[46–48]

Therefore, the participation of the $S_1 \rightarrow T_2 \rightarrow T_1$ pathway of relaxation can be ruled out. Other explanation of the weaker fluorescence in tetracene compared with 5-azatetracene would be stronger quenching by oxygen. However, our measurements of the fluorescence decay in the presence and absence of oxygen (Table S2) show small and comparable quenching in both compounds. Therefore, participation of the oxygen in the observed phenomenon can also be excluded. This is also supported by DFT calculations on the energy of interaction between tetracene and 5-azatetracene and oxygen (Figure S5 and Table S3).

Our explanation of the difference in PLQY in both compounds is as follows. In N-substituted heteroacenes, the singlet state consists of a lower-lying π-π* state followed by a weak n-π* state.[49] Depending on the various factors (solvent, position and number of N-atoms) the energy gap between these levels may vary.[50–53] DFT calculations show that 5-azatetracene has weak charge transfer properties while in tetracene there is no charge transfer. (Figure S6) The different charge distributions can influence the gap between n-π* and π-π* states.[54] Note

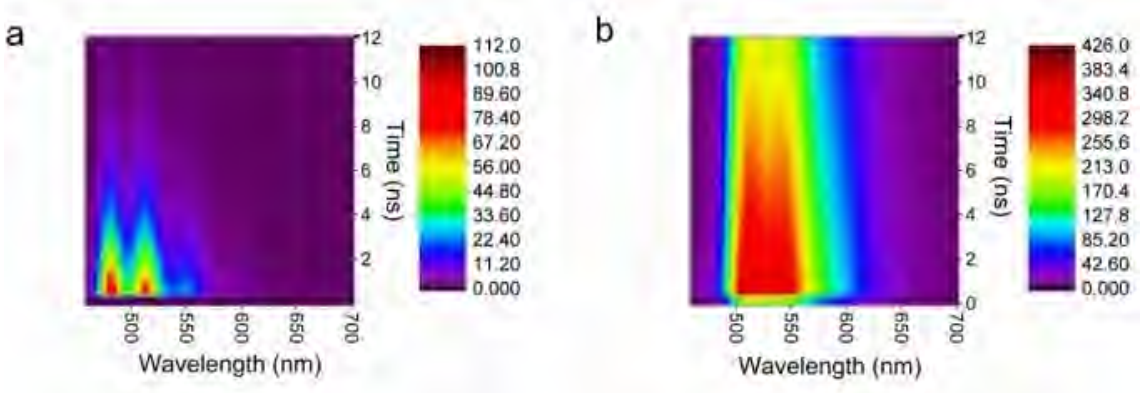

Figure 5. Fluorescence map of tetracene (a) and 5-azatetracene (b) in dichloromethane solution, $\lambda_{ex} = 380$ nm.

that in dibenzophenathroline derivatives emission arises from π-π* transitions.[55–57]

5-Azatetracene possesses large π-π conjugation, which leads to lowering of the π-π* state, as shown by the red-shifted fluorescence (Figure 5). Thus the energy gap between π-π* and n-π* is enlarged and, as a result, the excited state lifetime is prolonged due to the proximity effect,[58] which will in turn increase the PLQY.

The photoluminescence (PL) in solid state was investigated on thin films prepared by drop casting on glass slide from chloroform solution (Figure S2). The thin film emission spectra of tetracene exhibited two peaks at 536 and 521 nm; the first peak is blue shifted by 14 nm in comparison to that in solution. The thin film emission spectra of 5-azatetracene exhibited a peak at 538 nm, which is blue-shifted by 6 nm in comparison to that in solution.

Time resolved measurements of 5-azatetracene film prepared via vacuum evaporation on quartz at 343 K (Supporting Information, page 2) were performed by TCSPC technique at $\lambda_{ex} = 380$ nm; the resulting fluorescence kinetics and fluorescence map are shown in Figure S3. Lifetimes obtained from fit/deconvolution of TCSPC results of 5-azatetracene film are shown in Table S6. The emission of 5-azatetracene film exhibits biexponential decay: $\tau_1 = 70–90$ ps (70–80%), $\tau_2 = 240–400$ ps (20–30%). Biexponential decay is indicative of the inhomogeneous morphology of the film. In 5-azatetracene film, the fluorescence is strongly quenched compared with 5-azatetracene in dichloromethane solution ($\tau_f = 11$ ns).

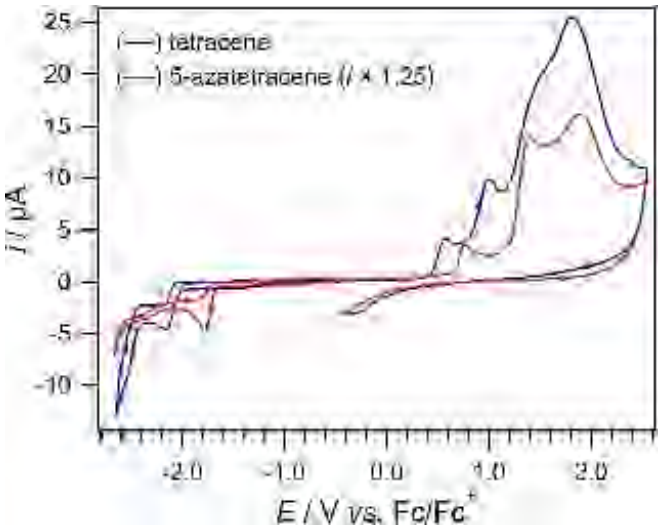

Figure 6. Cyclic voltammograms showing overall redox processes of 1 mM 5-azatetracene and tetracene in DCM containing 0.1 M nBu$_4$NPF$_6$ at a scan rate of 0.1 V s^{-1} and using a 1 mm diameter GC working electrode at 298 ± 2 K in a Faraday cage.

Electrochemical properties

The comparative electrochemical properties of 5-azatetracene and tetracene were studied by cyclic voltammetry (CV). The cyclic voltammetry experiments were performed in dry dichloromethane at room temperature with tetrabutylammonium hexafluorophosphate (nBu$_4$NPF$_6$) as a supporting electrolyte. The redox potentials were determined relative to ferrocene$^{0/+}$ (Fc/Fc$^+$). The CV plots obtained are shown in Figure 6 and the data from these are tabulated in Table 2.

Compounds **6** and **7** exhibited a single chemically irreversible reduction peak at −1.80 V and −2.15 V respectively. They also showed similar oxidation processes with three chemically irreversible oxidation waves. The first oxidation peak of 5-azatetracene was at +0.82 V and that of tetracene was at +0.56 V. Substitution with an electronegative nitrogen atom is expected to increase the electron affinity of the 5-azatetracene framework and so induce a shift of the reduction potentials to a less negative value. The HOMO-LUMO values were calculated from the following equations.[59]

$$E_{HOMO} = -[E_{(onset,\ ox\ vs.\ Fc+/Fc)} + 5.1](eV)$$

$$E_{LUMO} = -[E_{(onset,\ red\ vs.\ Fc+/Fc)} + 5.1](eV)$$

The HOMO-LUMO values estimated from the first oxidation/reduction peaks of 5-azatetracene and tetracene were −5.65 V/-3.5 V and −5.5 V/-3.1 V respectively. Thus, the electrochemical band gap for 5-azatetracene and tetracene were calculated to be 2.15 V and 2.4 V respectively. The electrochemical band gaps showed good agreement with the band gaps calculated from the absorption spectra (Table 1). The lower value of electrochemical band gap in 5-azatetracene is thus consistent with the bathochromic shift of its absorption peaks in its UV-vis spectra. The FMO energies obtained by DFT calculations (Figure S7 and Table S7) and the experimentally derived FMO energies of 5-azatetracene are both lower than for tetracene, indicating it has better stability than tetracene in electronic devices as well as in the excited state.

Both compounds showed complex electrochemistry with low chemical reversibility at scan rates of 0.1 V s^{-1}. In general, 1–2 reduction and 3–4 oxidation processes were observed. Aside from the overall redox processes, the chemical reversibility of the first reduction and oxidation waves were examined using

Table 2. Electrochemical data of 5-azatetracene (**6**) and tetracene (**7**).

Compound	E_{red}^1 [V][a]	E_{ox}^1 [V][a]	E_{ox}^2 [V]	E_{ox}^3 [V][a]	E_{onset}^{red1} [V]	E_{onset}^{ox1} [V]	HOMO [eV]	LUMO [eV]	E_g^{CV} [eV][b]
6	−1.80	+0.82	+1.35	+1.77	−1.60	+0.55	−5.65	−3.50	2.15
7	−2.15	+0.56	+1.01	+1.36	−2.00	+0.40	−5.50	−3.10	2.40

[a] Voltammetric peak potentials measured in dichloromethane solution. [b] Calculated from $E_g^{CV} = E_{LUMO} - E_{HOMO}$.

the assumption that the first electron-transfer reactions follow the EC mechanism (with E representing an electron transfer and C a chemical step reaction). Therefore, the processes that are observed at more positive or more negative potentials than the first oxidation or first reduction peaks respectively, are likely associated with decomposition products resulting from instability of the species formed via the initial electron transfer and not associated with reduction/oxidation of the primary compound. Figure 7a includes the results of the complete voltammetric reduction processes, showing that they appear chemically irreversible within the accessible potential window at a scan rate of 0.1 $V s^{-1}$. Figure 7b shows the results of CV experiments conducted to compare overall oxidation process to determine electron donor/acceptor ability of the compounds. The three to four oxidation peaks can be observed within the electrochemical potential window. The CVs in Figures 8a and 8b show that when the potential is reversed just after the first reduction process or first oxidation process, small reverse peaks are detected for tetracene but not for 5-azatetracene, suggesting that the first reduced and first oxidised states of tetracene were longer lived than those of 5-azatetracene.

When the electrochemical behaviour of 5-azatetracene and tetracene were compared, lower values of reduction potential and higher values for oxidation potentials for the 5-azatetracene were observed. This signifies that 5-azatetracene is a better electron acceptor, which is important in considering future possible applications in electronic devices.

Measurement of charge carrier mobilities using FETs

The electrical properties of 5-azatetracene were investigated by field-effect transistor measurements, which revealed the ambipolar nature of the charge transport (Figure 9). The extracted field-effect hole mobility $\mu_h = (2.3 \pm 0.4) \times 10^{-5}\ cm^2 V^{-1} s^{-1}$ was one order of magnitude higher than the electron mobility $\mu_e = (3.6 \pm 0.3) \times 10^{-6}\ cm^2 V^{-1} s^{-1}$. These results are in good agreement with literature values reported for similar organic solids: while the typical hole mobility for polyacene single crystals is around 1 $cm^2 V^{-1} s^{-1}$ (yet strongly dependent on the purity of the crystal), in disordered organic solids carrier mobilities are orders of magnitude smaller, typically around 10^{-3}–$10^{-6}\ cm^2 V^{-1} s^{-1}$.[60–62] The morphology of spin coated films is shown in Figure S4. Randomly oriented microcrystals 1–2 μm wide and 10 to 50 μm in length can be clearly distinguished. So far we have been unable to grow single crystals suitable for either X-Ray diffraction measurements or FET studies.

Conclusions

The Friedländer condensation of **8** with cyclohexanone and subsequent Pd catalysed aromatization allows the efficient synthesis of 5-azatetracene having a selectively embedded nitrogen atom. Introduction of an N atom considerably stabilized the FMOs as elucidated from the band gap calculation of absorption, as well as by electrochemical studies.

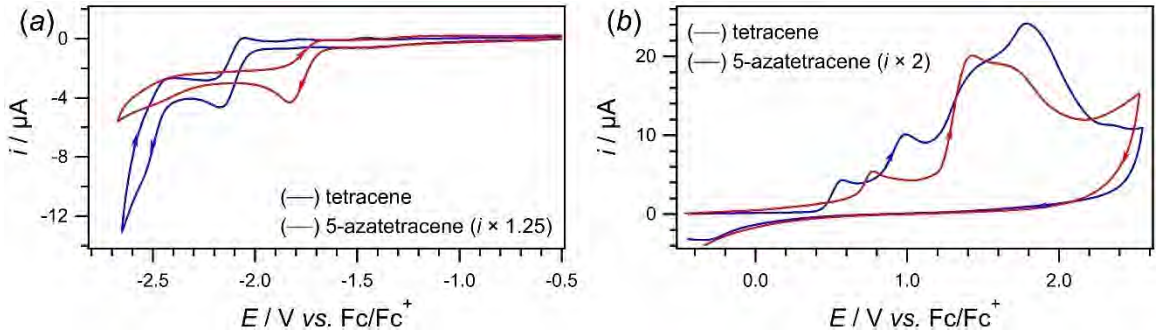

Figure 7. Cyclic voltammograms obtained in DCM containing 0.1 M nBu_4NPF_6 at a scan rate of 0.1 $V s^{-1}$ and using a 1 mm diameter GC working electrode at 298 ± 2 K in a Faraday cage. (a) Reduction processes of 1 mM 5-azatetracene and tetracene. (b) Oxidation processes of 1 mM 5-azatetracene and tetracene.

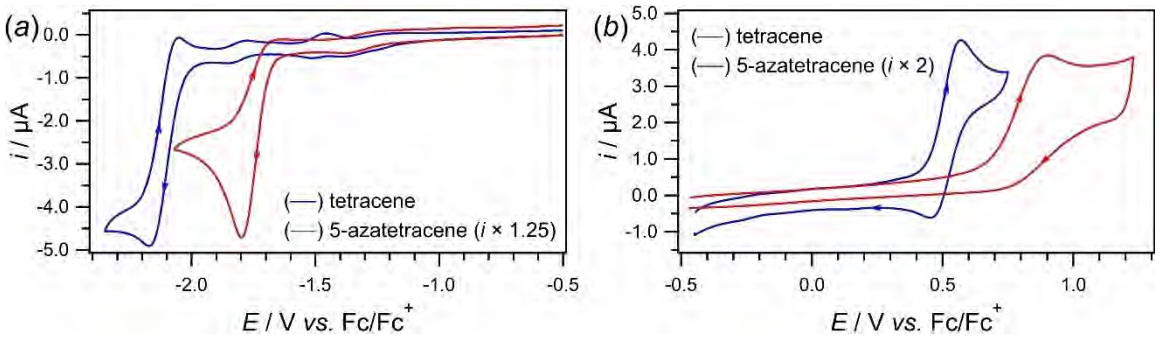

Figure 8. Comparison of (a) first reduction and (b) first oxidation process of 1 mM 5-azatetracene and tetracene. Cyclic voltammograms were recorded in DCM containing 0.1 M nBu_4NPF_6 at a scan rate of 0.1 $V s^{-1}$ and using a 1 mm diameter GC working electrode at 298 ± 2 K in a Faraday cage.

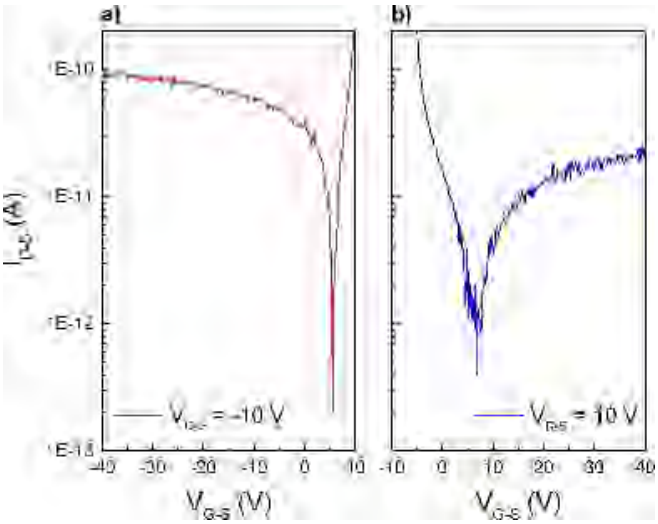

Figure 9. Representative p-type (a) and n-type (b) transfer characteristics measured at drain-source bias voltage of $V_{D-S} = \pm 10$ V. V_{G-S} is the applied gate-source voltage and I_{D-S} is the measured drain-source current.

5-azatetracene exhibited very strong fluorescence with much higher quantum yield value and better solubility in organic solvents including dichloromethane and chloroform in comparison to tetracene. Time-resolved studies showed that the better PL from the 5-azatetracene was due to an enlargement of the energy gap between the π-π* and n-π* transitions, which may also be true in other heteroacenes. This insight may be useful in explaining the behaviour of other heteroacenes and in designing new heteroacenes with optimal optical properties. The facile and high yielding synthesis in conjunction with the results of optoelectronic, electrochemical and electrical studies indicate that 5-azatetracene is worth further investigation as a potential candidate for applications in organic electronic devices.

Experimental Section

General: 3-Amino-napthoic acid and other reagents were obtained from Sigma-Aldrich and used without further purification. Chromatographic purification was performed as flash chromatography with silica gel (40–65 μm) and solvents indicated as eluent with 0.1–0.5 bar pressure. For quantitative flash chromatography, technical grades solvents were utilized. Analytical thin-layer chromatography (TLC) was performed on silica gel 60 μm F254 TLC glass plates. Visualization was accomplished with UV light. Melting point measurements were performed using a PerkinElmer DSC 8500. Infrared spectra were recorded using a PerkinElmer FT-IR Spectrometer Frontier with KBr pellets in the 4000–400 cm^{-1} region.". Proton and carbon nuclear magnetic resonance spectra (^{1}H NMR and ^{13}C NMR) were recorded on Bruker AVANCE 400 MHz spectrometers with solvent resonances as the internal standard (^{1}H NMR: $CDCl_3$ at 7.26 ppm; ^{13}C NMR: $CDCl_3$ at 77.0 ppm). The accurate mass analyses were run in ESI mode on a double focusing magnetic sector mass spectrometer at a mass resolution of 10 000 using PFK (perfluorokerosene) as an internal calibrant or in ESI mode using a hybrid linear ion trap/orbitrap tandem mass spectrometer.

UV-visible spectroscopy was performed on a Shimadzu UV-2700 spectrophotometer. Fluorescence spectra in solution and in solid state (thin film) were measured on a Cary Eclipse spectrophotometer and Fluorolog spectrofluorometer (Horiba) respectively. Quantum yields (Φ) were obtained by the absolute method using Quantum Efficiency Measurement System QE-2000 (Otsuka Electronics Co., Ltd). The given Φ values for solutions in chloroform are average values of three independent measurements. Voltammetric measurements were performed using a Metrohm Autolab PGSTAT302 N potentiostat in a three-electrode setup. A 1 mm diameter planar disk glassy carbon disk (GC, Cypress Systems) was used as a working electrode in conjunction with a platinum wire counter electrode (Metrohm) and Ag wire reference electrode connected to the test solution via a salt bridge containing 0.5 M tetra-n-butylammonium hexafluorophosphate (nBu$_4$NPF$_6$) in DCM. All voltammetric experiments were conducted under an argon atmosphere, at room temperature in a Faraday cage. Prior to each scan, the working electrode was cleaned by polishing with alumina oxide (grain size 0.3 μm) slurry on a Buehler Ultra-pad polishing cloth, rinsing with acetone, and then dried with a lint free tissue. In accordance with IUPAC recommendations, the absolute potentials were calibrated using Fc as an internal reference, which was added to the test solution at the end of the measurements. Thin film morphology was characterized using SEM (FEI Helios NanoLab DualBeam).

Experimental Details of Synthesis

(3-aminonaphthalen-2-yl)methanol: To a solution of LAH (1 M in THF) (80 mL, 80 mmol) cooled at −10 °C, a solution of 3-amino-2-naphthoic acid (**9**, 5.0 g, 26.7 mmol) in anhydrous THF (100 mL) was added dropwise under argon atmosphere. The reaction mixture was warmed slowly to ambient temperature and stirred at room temperature for 4 h. The reaction was quenched slowly with saturated aqueous Na_2SO_4 (50 mL) at −10 °C and then warmed to ambient temperature. Afterwards it was diluted with EtOAc and filtered over celite. The filtrate was successively washed with water and brine solution, dried ($MgSO_4$) and concentrated. The residue was purified by column chromatography on silica gel (ethyl acetate/DCM/hexane 7:2:1) to afford (3-aminonaphthalen-2-yl) methanol as an off-white solid (3.4 g, 74%).^{1}H NMR (400 MHz, $CDCl_3$) δ 7.68 (d, J = 8.0 Hz, 1H), 7.62–7.56 (m, 2H), 7.40–7.34 (m, 1H), 7.25–7.20 (m, 1H), 7.03 (s, 1H), 4.84 (s, 2H).

3-amino-2-naphthaldehyde (8): To a solution of (3-aminonaphthalen-2-yl) methanol (3.0 g, 17.3 mmol) in anhydrous CH_2Cl_2 (150 mL) was added MnO_2 (6.0 g, 69.3 mmol) in five portions under an argon atmosphere. The reaction mixture was stirred at room temperature for 8 h. It was then filtered through celite and the filter cake was washed with CH_2Cl_2 (DCM, 50 mL). The solvent was removed under reduced pressure, and the brown residue was purified by column chromatography on silica gel (ethyl acetate/DCM/hexane 15:15:70), to afford **8** as an off-white solid (1.4 g, 47%).^{1}H NMR (400 MHz, $CDCl_3$) δ 10.09 (s, 1H), 8.07 (s, 1H), 7.76 (d, J = 8.0 Hz, 1H), 7.54 (d, J = 8.0 Hz, 1H), 7.49–7.41 (m, 1H), 7.25–7.17 (m, 1H), 6.92 (s, 1H), 5.77 (s, 2H).

1,2,3,4-tetrahydrobenzo[b]acridine (10): To a solution of cyclohexanone (1.4 g, 14.0 mmol) in ethanol (100 mL) at room temperature was added **8** (600 mg, 3.5 mmol) followed by KOH (1.2 g, 21.0 mmol). The reaction mixture was heated under reflux for 2 h. The reaction mixture was cooled and the ethanol was evaporated under reduced pressure. The residue was diluted with water (100 mL) and extracted with DCM (2 × 50 mL). The organic extracts were combined, dried ($MgSO_4$), filtered and concentrated. The resulting yellow residue was purified by column chromatography on silica gel (ethyl acetate//DCM/hexane 25:20:55) to afford **10** as a light-yellow solid (675 mg, 83%). ^{1}H NMR (400 MHz, $CDCl_3$) δ 8.53 (s, 1H), 8.14 (s, 1H), 8.05–7.97 (m, 1H), 7.96–7.88 (m, 1H), 7.82 (s, 1H),

7.47–7.39 (m, 2H), 3.15 (t, J = 8.0 Hz, 2H), 2.94 (t, J = 8.0 Hz, 2H), 2.02–1.94 (m, 2H), 1.91–1.83 (m, 2H); ^{13}C NMR (100 MHz, $CDCl_3$) δ 160.8, 143.3, 134.2, 133.3, 131.2, 130.7, 128.3, 127.8, 125.9, 125.6, 125.5, 125.2 (2), 33.9, 29.4, 23.0, 22.8.

5-azatetracene (6): N_2 (g) was bubbled through a mixture of **10** (180 mg, 0.77 mmol) and 10% Pd/C (225 mg) in nitrobenzene (5 mL) in a Schlenk flask at room temperature for 5 min. The flask was capped and the reaction mixture was stirred at 150 °C for 4 h. The reaction mixture was cooled to room temperature Pd/C was filtered off. The solvent was evaporated under reduced pressure, and the residue was purified by column chromatography on silica gel (ethyl acetate//DCM/hexane 25:25:50) to afford **6** as a light brown solid (69 mg, 39%). Mp: 221 °C. ^{1}H NMR (400 MHz, $CDCl_3$) δ 9.01 (s, 1H), 8.90 (s, 1H), 8.66 (s, 1H), 8.25–8.19 (m, 1H), 8.12–8.07 (m, 1H), 8.05–7.97 (m, 2H), 7.78–7.73 (m, 1H), 7.51–7.43 (m, 3H); ^{13}C NMR (100 MHz, $CDCl_3$) δ 150.4, 145.6, 136.6, 134.7, 131.5, 130.7, 129.5, 128.6, 128.4, 128.2, 126.9 (2), 126.3, 125.7, 125.3, 125.2; IR (KBr, cm^{-1}): 3044, 2927, 1595, 1529, 1376, 1124, 918, 742; UV-vis (DCM), λ_{max} (nm) 534 (ε_{max} $0.12\times10^4\ M^{-1}cm^{-1}$), 397 ($2.82\times10^4\ M^{-1}cm^{-1}$), 376 ($0.91\times10^4\ M^{-1}cm^{-1}$); HRMS (ESI) m/z calcd for $C_{17}H_{12}N\ [M+H]^+ = 230.0964$; found 230.0963.

Acknowledgements

We acknowledge funding from the Singapore Ministry of Education through the Academic Research Fund Tier 1 grant RG117/15 and Tier 2 grant MOE2019-T2-1-085. We thank Madame Wong Lai Kwai at Chemistry Department, National University of Singapore for performing the high resolution mass spectra. We thank Ms Xiaoxuan Chen and Associate Professor Handong Sun from SPMS for measuring the photoluminescence quantum yields. We thank Ms Wenjun Ni for useful discussions.

Conflict of Interest

There are no conflicts to declare

Keywords: cyclic voltammetry · field-effect transistor · Friedlander condensation · nitrogen heterocycles · photoluminescence spectroscopy · time resolved measurements

[1] J. E. Anthony, *Chem. Rev.* **2006**, *106*, 5028–5048.
[2] M. Bendikov, F. Wudl, D. F. Perepichka, *Chem. Rev.* **2004**, *104*, 4891–4946.
[3] T. Hasegawa, J. Takeya, *Sci. Technol. Adv. Mater.* **2009**, *10*, 024314.
[4] J. E. Anthony, *Angew. Chem. Int. Ed.* **2008**, *47*, 452–483; *Angew. Chem.* **2008**, *120*, 460–492.
[5] Q. Ye, C. Chi, *Chem. Mater.* **2014**, *26*, 4046–4056.
[6] C. Du, Y. Guo, J. Chen, H. Liu, Y. Liu, S. Ye, K. Lu, J. Zheng, T. Wu, Y. Liu, Z. Shuai, G. Yu, *J. Phys. Chem. C* **2010**, *114*, 10565–10571.
[7] B. Wex, B. R. Kaafarani, D. C. Neckers, *J. Org. Chem.* **2004**, *69*, 2197–2199.
[8] G. Li, Y. Wu, J. Gao, C. Wang, J. Li, H. Zhang, Y. Zhao, Y. Zhao, Q. Zhang, *J. Am. Chem. Soc.* **2012**, *134*, 20298–20301.
[9] P. G. Campbell, A. J. V. Marwitz, S.-Y. Liu, *Angew. Chem. Int. Ed.* **2012**, *51*, 6074–6092; *Angew. Chem.* **2012**, *124*, 6178–6197.
[10] F. L. Geyer, V. Brosius, U. H. F. Bunz, *J. Org. Chem.* **2015**, *80*, 12166–12176.
[11] X.-Y. Wang, F.-D. Zhuang, R.-B. Wang, X.-C. Wang, X.-Y. Cao, J.-Y. Wang, J. Pei, *J. Am. Chem. Soc.* **2014**, *136*, 3764–3767.
[12] X.-Y. Wang, J.-Y. Wang, J. Pei, *Chem. Eur. J.* **2015**, *21*, 3528–3539.
[13] S. Hahn, F. L. Geyer, S. Koser, O. Tverskoy, F. Rominger, U. H. F. Bunz, *J. Org. Chem.* **2016**, *81*, 8485–8494.
[14] T. Zheng, Z. Cai, R. Ho-Wu, S. H. Yau, V. Shaparov, T. Goodson, L. Yu, *J. Am. Chem. Soc.* **2016**, *138*, 868–875.
[15] G. Long, X. Yang, W. Chen, M. Zhang, Y. Zhao, Y. Chen, Q. Zhang, *Phys. Chem. Chem. Phys.* **2016**, *18*, 3173–3178.
[16] Q. Miao, T.-Q. Nguyen, T. Someya, G. B. Blanchet, C. Nuckolls, *J. Am. Chem. Soc.* **2003**, *125*, 10284–10287.
[17] M. Tadokoro, S. Yasuzuka, M. Nakamura, T. Shinoda, T. Tatenuma, M. Mitsumi, Y. Ozawa, K. Toriumi, H. Yoshino, D. Shiomi, K. Sato, T. Takui, T. Mori, K. Murata, *Angew. Chem. Int. Ed.* **2006**, *45*, 5144–5147; *Angew. Chem.* **2006**, *118*, 5268–5271.
[18] A. L. Appleton, S. M. Brombosz, S. Barlow, J. S. Sears, J.-L. Bredas, S. R. Marder, U. H. F. Bunz, *Nat. Commun.* **2010**, *1*, 91.
[19] U. H. F. Bunz, J. U. Engelhart, B. D. Lindner, M. Schaffroth, *Angew. Chem. Int. Ed.* **2013**, *52*, 3810–3821; *Angew. Chem.* **2013**, *125*, 3898–3910.
[20] Z. Liang, Q. Tang, R. Mao, D. Liu, J. Xu, Q. Miao, *Adv. Mater.* **2011**, *23*, 5514–5518.
[21] Y.-Y. Liu, C.-L. Song, W.-J. Zeng, K.-G. Zhou, Z.-F. Shi, C.-B. Ma, F. Yang, H.-L. Zhang, X. Gong, *J. Am. Chem. Soc.* **2010**, *132*, 16349–16351.
[22] C. Wang, J. Zhang, G. Long, N. Aratani, H. Yamada, Y. Zhao, Q. Zhang, *Angew. Chem. Int. Ed.* **2015**, *54*, 6292–6296; *Angew. Chem.* **2015**, *127*, 6390–6394.
[23] O. Tverskoy, F. Rominger, A. Peters, H.-J. Himmel, U. H. F. Bunz, *Angew. Chem. Int. Ed.* **2011**, *50*, 3557–3560; *Angew. Chem.* **2011**, *123*, 3619–3622.
[24] U. H. F. Bunz, *Acc. Chem. Res.* **2015**, *48*, 1676–1686.
[25] P. Biegger, S. Stolz, S. N. Intorp, Y. Zhang, J. U. Engelhart, F. Rominger, K. I. Hardcastle, U. Lemmer, X. Qian, M. Hamburger, U. H. F. Bunz, *J. Org. Chem.* **2015**, *80*, 582–589.
[26] M. Märken, B. D. Lindner, A. L. Appleton, F. Rominger, U. H. Bunz, *Pure Appl. Chem.* **2014**, *86*, 483–488.
[27] J. U. Engelhart, B. D. Lindner, O. Tverskoy, F. Rominger, U. H. F. Bunz, *Chem. Eur. J.* **2013**, *19*, 15089–15092.
[28] J. U. Engelhart, O. Tverskoy, U. H. F. Bunz, *J. Am. Chem. Soc.* **2014**, *136*, 15166–15169.
[29] Y.-D. Zhang, Y. Wu, Y. Xu, Q. Wang, K. Liu, J.-W. Chen, J.-J. Cao, C. Zhang, H. Fu, H.-L. Zhang, *J. Am. Chem. Soc.* **2016**, *138*, 6739–6745.
[30] A. V. Lunchev, V. C. Hendrata, A. Jaggi, S. A. Morris, R. Ganguly, X. Chen, H. Sun, A. C. Grimsdale, *J. Mater. Chem. C* **2018**, *6*, 3715–3721.
[31] A. V. Lunchev, S. A. Morris, R. Ganguly, A. C. Grimsdale, *Chem. Eur. J.* **2019**, *25*, 1819–1823.
[32] J. Zhang, Y. Chen, X. Chen, X. Zheng, W. Cao, J. Chen, M. Zhang, *Tetrahedron* **2014**, *70*, 5820–5827.
[33] M.-L. Tan, S. Tong, S.-K. Hou, J. You, M.-X. Wang, *Org. Lett.* **2020**, *22*, 5417–5422.
[34] Y. Jahng, M. Karim, *Tetrahedron* **2016**, *72*, 199–204.
[35] E. Sanchez-Diez, D. L. Vesga, E. Reyes, U. Uria, L. Carrillo, J. L. Vicario, *Org. Lett.* **2016**, *18*, 1270–1273.
[36] T. W. Bell, J. Liu, *J. Am. Chem. Soc.* **1988**, *110*, 3673–3674.
[37] E. C. Riesgo, X. Jin, R. P. Thummel, *J. Org. Chem.* **1996**, *61*, 3017–3022.
[38] T. G. Majewicz, P. Caluwe, *J. Org. Chem.* **1975**, *40*, 3407–3410.
[39] S. Chackal, R. Houssin, J.-P. Hénichart, *J. Org. Chem.* **2002**, *67*, 3502–3505.
[40] C.-S. Jia, Z. Zhang, S.-J. Tu, G.-W. Wang, *Org. Biomol. Chem.* **2006**, *4*, 104–110.
[41] T. A. Shoker, K. I. Ghattass, J. C. Fettinger, M. J. Kurth, M. J. Haddadin, *Org. Lett.* **2012**, *14*, 3704–3707.
[42] N. Nakamichi, Y. Kawashita, M. Hayashi, *Org. Lett.* **2002**, *4*, 3955–3957.
[43] C. Wetzel, A. Mishra, E. Mena-Osteritz, A. Liess, M. Stolte, F. Würthner, P. Bäuerle, *Org. Lett.* **2014**, *16*, 362–365.
[44] J. J. Burdett, A. M. Müller, D. Gosztola, C. J. Bardeen, *J. Chem. Phys.* **2010**, *133*, 144506.
[45] F. Lewitzka, H.-G. Löhmannsröben, *Z. Phys. Chem.* **1986**, *150*, 69-86.
[46] S. Arnold, W. B. Whitten, *J. Chem. Phys.* **1981**, *75*, 1166–1169.
[47] E. S. Kadantsev, M. J. Stott, A. Rubio, *J. Chem. Phys.* **2006**, *124*, 134901.
[48] H. H. Heinze, A. Görling, N. Rösch, *J. Chem. Phys.* **2000**, *113*, 2088–2099.
[49] J. Thusek, M. Hoffmann, O. Hübner, O. Tverskoy, U. H. F. Bunz, A. Dreuw, H.-J. Himmel, *Chem. Eur. J.* **2019**, *25*, 15147–15154.
[50] G. M. Badger, I. S. Walker, *J. Chem. Soc.* **1956**, 122–126.
[51] W. S. Struve, J. H. Hedstrom, C. G. Morgante, A. K. Jameson, E. C. Lim, *J. Chem. Phys.* **1983**, *78*, 7006–7008.
[52] E. Tervola, K. N. Truong, J. S. Ward, A. Priimagi, K. Rissanen, *RSC Adv.* **2020**, *10*, 29385–29393.

[53] A. Grabowska, B. Pakuła, *Photochem. Photobiol.* **1969**, *9*(4), 339–350.
[54] V. Botti, U. Mazzucato, M. Sindler-Kulyk, A. Spalletti, *J. Photochem.* **2017**, *333*, 33–39.
[55] D. Tzalis, Y. Tor, *Tetrahedron Lett.* **1995**, *36*, 6017–6020.
[56] D. R. Maulding, B. G. Roberts, *J. Org. Chem.* **1969**, *34*, 1734–1736.
[57] M. T. Miller, T. B. Karpishin, *Inorg. Chem.* **1999**, *38*, 5246–5249.
[58] W. A. W. Jr, E. C. Lim, *J. Chem. Phys.* **1978**, *68*, 433–454.
[59] C. M. Cardona, W. Li, A. E. Kaifer, D. Stockdale, G. C. Bazan, *Adv. Mater.* **2011**, *23*, 2367–2371.
[60] W. Mycielski, *J. Non-Cryst. Solids* **1980**, *37*, 267–271.
[61] M. Schwoerer, H. C. Wolf, *Organic molecular solids*, John Wiley & Sons, **2007**.
[62] Y. Xia, V. Kalihari, C. D. Frisbie, N. K. Oh, J. A. Rogers, *Appl. Phys. Lett.* **2007**, *90*, 162106.

Manuscript received: June 16, 2021
Revised manuscript received: July 26, 2021
Accepted manuscript online: August 17, 2021
Version of record online: August 26, 2021